

Prediction of rise velocity of a liquid Taylor bubble in a vertical tube

T. K. Mandal, G. Das, and P. K. Das

Citation: *Physics of Fluids* (1994-present) **19**, 128109 (2007); doi: 10.1063/1.2824414

View online: <http://dx.doi.org/10.1063/1.2824414>

View Table of Contents: <http://scitation.aip.org/content/aip/journal/pof2/19/12?ver=pdfcov>

Published by the *AIP Publishing*

Articles you may be interested in

[Terminal velocity of a bubble in a vertically vibrated liquid](#)

Phys. Fluids **26**, 053301 (2014); 10.1063/1.4873416

[Analytical solution of the problem of the rise of a Taylor bubble](#)

Phys. Fluids **25**, 053302 (2013); 10.1063/1.4803878

[The stability of a bubble in a weakly viscous liquid subject to an acoustic traveling wave](#)

Phys. Fluids **21**, 022104 (2009); 10.1063/1.3076932

[Path instability of rising spheroidal air bubbles: A shape-controlled process](#)

Phys. Fluids **20**, 061702 (2008); 10.1063/1.2940368

[A study of velocity discontinuity for single air bubbles rising in an associative polymer](#)

Phys. Fluids **18**, 121510 (2006); 10.1063/1.2397011



Prediction of rise velocity of a liquid Taylor bubble in a vertical tube

T. K. Mandal and G. Das

Department of Chemical Engineering, Indian Institute of Technology, Kharagpur-723302, India

P. K. Das^{a)}

Department of Mechanical Engineering, Indian Institute of Technology, Kharagpur-723302, India

(Received 20 June 2007; accepted 29 October 2007; published online 28 December 2007)

In the present study, a theoretical analysis has been performed to predict rise velocity of liquid Taylor bubbles. The viscous potential flow analysis has been adopted for this purpose. The results have revealed the importance of nose shape. This has been quantified by a shape factor. A method for estimating this factor has also been proposed. © 2007 American Institute of Physics.

[DOI: 10.1063/1.2824414]

In two phase terminology, Taylor bubbles are elongated bubbles whose length exceeds 1.5 times the tube diameter or its diameter is greater than 60% of the tube diameter.^{1,2} These bubbles are axisymmetric in vertical pipes and are comprised of a spherical nose and a cylindrical tail. The photograph of a Taylor bubble formed when a volume of lighter liquid rises through a stationary column of heavier liquid is shown in Fig. 1(a). These have been termed as liquid Taylor bubbles or LTB in the present study.

Several attempts have been made to propose theoretical models for the prediction of shape and rise velocity of Taylor bubbles in gas-liquid cases. However, due to the complex hydrodynamics, the development of a generalized solution taking care of all the physical and geometrical parameters is formidable. Therefore, several researchers have proposed solutions on the basis of different simplifying assumptions. The assumption of inviscid flow past the nose of the bubble^{3,4} has provided the first and probably the simplest analysis of the problem. Garabedian,⁵ Goldsmith and Mason,⁶ Brown,⁷ and Reinelt⁸ have improved this analysis by incorporating the viscosity of the primary fluid (through which the bubble passes). A number of researchers have incorporated the effect of interfacial tension empirically (Clift, *et al.*,⁹ Wallis,^{10,11} Tomiyama *et al.*,² Viana *et al.*¹²) as well as theoretically (Bretherton,¹³ Tung and Parlange,¹⁴ Vanden-Broeck,¹⁵ Nickens and Yannitell,¹⁶ Couet and Strumolo¹⁷). Recently, Joseph¹⁸ has proposed the viscous potential flow analysis where he has introduced interfacial tension into the normal stress balance for prediction of rise velocity of a spherical cap bubble in a gas-liquid system. He has shown that the influence of interfacial tension on rise velocity is dependent on the sphericity of the bubble. The viscous potential flow theory has further been extended by Funada *et al.*¹⁹ to analyze the rise of an ellipsoidal cap bubble in a round tube.

On the other hand, little attention has so far been paid to investigate the dynamics of Taylor bubbles in liquid-liquid systems. We could trace the only work due to Zukoski¹ who has performed some experiments to note the influence of

fluid properties, tube diameter, and tube inclination on velocity and shape of long bubbles in liquid-liquid systems.

In the present work, the analysis by Joseph¹⁸ has been extended to liquid-liquid systems for prediction of rise velocity of a liquid Taylor bubble. The shape factor defined as “deviation from sphericity” has been calculated from the image analysis of the nose of a LTB. The results of the analysis have further been validated with experimental data.

Since the nose of the Taylor bubble is hemispherical (Fig. 1) and the nose governs the rise velocity of a Taylor bubble, it is felt that the analysis by Joseph¹⁹ for cap bubbles can be extended to predict the rise velocity of a Taylor bubble in liquid-liquid systems. For the analysis, the geometry of the bubble nose is shown in Fig. 1(b). The figure shows a stationary spherical cap held by the primary liquid falling from infinity at the rise velocity (U) of the bubble. The origin of the coordinate axis is at the stagnation point \hat{s} . At this condition, the surface of the cap is given by

$$z = -h(r, \theta) = -[R - r(\theta)\cos\theta], \quad (1)$$

where

$$r(\theta) = R(1 + s\theta^2) \quad (2)$$

and the deviation of the free surface from perfect sphericity is expressed as

$$s = r''(0)/D. \quad (3)$$

In Eq. (3), D is the tube diameter. Near the stagnation point $\theta=0$ and $r(\theta)=R$ which is constant for a perfectly spherical bubble.

Taking the queue from Joseph's analysis, the velocity field on the primary and secondary liquid has been derived from a potential $u=\nabla\phi$, where $\nabla^2\phi=0$. The velocity at $z=\infty$ is $-U$ (against Z) and $g=-e_zg$. For steady flow,

$$\rho u \cdot \nabla u = -\nabla p - \rho e_z g = -\nabla \Gamma, \quad (4)$$

where $\Gamma = p + \rho g z$.

The Bernoulli function in the primary liquid is obtained from Eq. (4) as

$$\rho_p \frac{|u_p|^2}{2} + \Gamma_p = \frac{\rho_p U^2}{2}. \quad (5)$$

^{a)} Author to whom correspondence should be addressed.
Telephone +91 3222 282916. Fax: +91 3222 255303.
Electronic mail: pkd@mech.iitkgp.ernet.in.

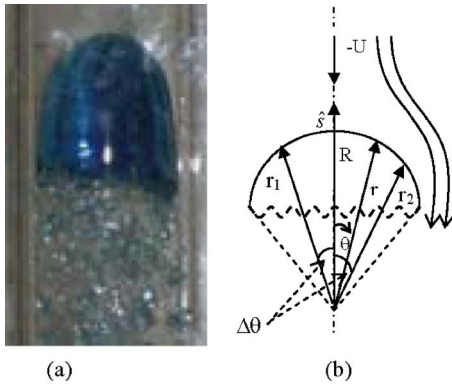


FIG. 1. (Color online) Rising LTB in a vertical tube. (a) Photograph and (b) geometrical details.

Similarly for the secondary liquid, Bernoulli function is

$$\frac{\rho_s |u_s|^2}{2} + \Gamma_s = C_s, \quad (6)$$

where C_s is an unknown constant and suffixes p and s denotes the primary and secondary fluid, respectively.

The normal stress balance on the bubble interface is as follows:

$$-[[p]] + 2[[\mu n \cdot D[u]]] \cdot n + \frac{2\sigma}{r(\theta)} = 0, \quad (7)$$

where $[[\cdot]] = (\cdot)_s - (\cdot)_p$ is evaluated on $r(\theta) = R(1 + s\theta^2)$. n is the unit normal to the interface directed from the secondary phase (bubble phase) to the primary liquid phase, τ is the normal stress, and σ is the surface tension force.

Replacing p by Γ [from Eq. (4)] and normal stress by normal strain, Eq. (7) becomes

$$-[[\Gamma]] - [[\rho]]gh + 2\left[\left[\mu \frac{\partial u_n}{\partial n}\right]\right] + \frac{2\sigma}{r} = 0, \quad (8)$$

where $z = -h$ on the free surface.

The potential flow analysis is applicable near the stagnation point of the bubble, i.e., at the tip of the nose, which is nearly spherical. From this consideration and ignoring the higher order terms (greater than θ^2) u_r , u_θ , $\partial u_n / \partial n$, and h have been calculated for the primary liquid at the free surface as

$$u_r = -3Us\theta^2, \quad (9)$$

$$u_\theta = \frac{3}{2}U\theta, \quad (10)$$

$$\frac{\partial u_n}{\partial n} = \frac{\partial u_r}{\partial r} = -3\frac{U}{R}\left[1 - \left(4s + \frac{1}{2}\right)\theta^2\right], \quad (11)$$

and

$$h = R\left(\frac{1}{2} - s\right)\theta^2. \quad (12)$$

Considering that the velocity gradient of the secondary liquid in the bubble phase has a negligible influence on the

rise velocity, the potential of the secondary liquid has not been accounted for. The simplifying form of Eq. (6) on the bubble surface is, therefore,

$$\Gamma_s = C_s. \quad (13)$$

Similarly Eq. (5) becomes

$$\Gamma_p = -\frac{9}{8}\rho_p U^2 \theta^2 + \rho_p \frac{U^2}{2}. \quad (14)$$

Using Eqs. (9)–(14), Eq. (8) is rearranged as

$$\left[-\frac{9}{8}\rho_p U^2 + (\rho_p - \rho_s)\left(\frac{1}{2} - s\right)gR - 6\frac{\mu_p U}{R}\left(4s + \frac{1}{2}\right) - 2\frac{s\sigma}{R}\right]\theta^2 + \left[\rho_p \frac{U^2}{2} + 6\frac{\mu_p U}{R} + \frac{2\sigma}{R}\right] = C_s. \quad (15)$$

Comparing the constant term and the coefficient of θ^2 from both sides we get

$$\left[\rho_p \frac{U^2}{2} + 6\frac{\mu_p U}{R} + \frac{2\sigma}{R}\right] = C_s, \quad (16)$$

and

$$\left[\frac{9}{8}\rho_p U^2 - (\rho_p - \rho_s)\left(\frac{1}{2} - s\right)gR + 6\frac{\mu_p U}{R}\left(4s + \frac{1}{2}\right) + 2\frac{s\sigma}{R}\right] = 0, \quad (17)$$

$$\begin{aligned} \therefore U = & -\frac{8}{3}\frac{\nu}{D}(1 + 8s) \\ & + \frac{\sqrt{2}}{3}\sqrt{(1 - 2s)gD\frac{\rho_p - \rho_s}{\rho_p} - \frac{16\sigma s}{\rho_p D} + \frac{32\nu^2}{D^2}(1 + 8s)^2}, \end{aligned} \quad (18)$$

where ν is the kinematics viscosity. The above equation can be expressed in terms of Froude number, gravity Reynolds number, Eotvos number as

$$\begin{aligned} \text{Fr} = & -\frac{8(1 + 8s)}{3\text{Re}_G} \\ & + \frac{\sqrt{2}}{3}\sqrt{(1 - 2s)\frac{\rho_p - \rho_s}{\rho_p} - \frac{16s}{\text{Eo}} + \frac{32}{\text{Re}_G^2}(1 + 8s)^2}, \end{aligned} \quad (19)$$

where Froude number, $\text{Fr} = U/\sqrt{gD}$, gravity Reynolds number, $\text{Re}_G = \sqrt{gD^3}/\nu$, and Eotvos number $\text{Eo} = \rho g D^2 / \sigma$.

Wallis¹² has shown that the rise velocity of long bubbles can be characterized by Fr , Re_G , and Eo only. Equation (19) also provides a similar expression for liquid Taylor bubbles providing a prior estimate of s is known. The equation further shows that the effect of interfacial tension on rise velocity is associated with s and the effect vanishes when s equals zero. This indicates that the interfacial tension comes into account in the prediction of rise velocity only when bubbles are deformed.

From the geometrical definition of the second derivative, s can be expressed as

TABLE I. Comparison of predicted results with experimental results.

Liquid pair	$D (\times 10^2 \text{ m})$	s	Predicted Fr	Expt. Fr	% Error
Kerosene bubble in water	1.2	0.082	0.0465	0.051	-1.374
	1.76	0.12	0.1022	0.101	1.018
	2.57	0.15	0.1347	0.139	3.287
	3.58	0.18	0.1449	0.142	3.455
	4.61	0.21	0.1446	0.153	5.627
Kerosene bubble in brine	1.2	0.158	0.1240	0.115	-3.951
	1.76	0.208	0.1482	0.154	5.421
	2.57	0.21	0.1831	0.186	1.369
	3.58	0.23	0.1875	0.187	-0.098
	4.61	0.25	0.1849	0.187	1.727
Benzene bubble in water	1.2	0.0329	0.0267	0.019	-4.926
	1.76	0.045	0.0943	0.081	-4.663
	2.57	0.07	0.1084	0.111	1.174
	3.58	0.109	0.1091	0.118	4.904
	4.61	0.14	0.1109	0.120	4.524
Cyclohexane bubble in water	1.2	0.0604	0.0641	0.039	-4.220
	1.76	0.0824	0.1281	0.101	-2.506
	2.57	0.12496	0.1395	0.147	5.343
	3.58	0.1579	0.1499	0.163	5.547
	4.61	0.1789	0.1552	0.160	3.826
2, Heptanone bubble in water	1.2	0.11	0.0539	0.111	-3.083
	1.76	0.13	0.1207	0.149	-5.938
	2.57	0.148	0.1439	0.149	-3.575
	3.58	0.17	0.1499	0.152	-1.557
	4.61	0.191	0.1496	0.147	-1.323

$$s = \frac{(r_1 + r_2) - 2R}{(\Delta\theta)^2 D}, \quad (20)$$

where r_1 , r_2 , and R are the radii and $\Delta\theta$ is the angle as shown in Fig. 1(b). The aforementioned parameters can be obtained from an analysis of the actual profile of the nose of a Taylor bubble. For this purpose, the photographs of a Taylor bubble have been captured using a digital camera (SONY DSC-F717) and analyzed by Image-Pro Plus software (version 5.1). The above parameters have been measured and substituted in Eq. (20). The shape factor thus obtained is used in Eq. (19) to calculate the Froude number. The results of the calculations are listed in Table I. The corresponding experimental values as obtained from the present work are also provided for a comparative study. The experiments have been conducted in five different diameters of tube ranging from 0.012 m to 0.0461 m and five liquid pairs whose names and physical properties are listed in Table II. The % deviations shown in the table are based on the experimental value of rise velocity. They lie within $\pm 6\%$ for all the cases, thus hinting at the validity of the proposed analysis.

A further interest was felt to note the improvement of the present analysis over the model by Joseph.¹⁸ A close observation of Eq. (19) and the expression obtained from the previous model indicates that Eq. (19) has an additional term $(1 - \rho_s/\rho_p)$ to account for the density difference between the two fluids. Moreover in the absence of further information Joseph¹⁸ assumed $s=0$ to calculate rise velocity and vali-

dated the values thus obtained with experimental data.

Accordingly, three cases have been considered for the comparative study. These include (i) $s \neq 0$ and $\rho_s=0$, i.e., the shape factor exists, which modifies Eq. (19) as

$$\text{Fr} = -\frac{8(1+8s)}{3 \text{Re}_G} + \frac{\sqrt{2}}{3} \sqrt{(1-2s) - \frac{16s}{\text{Eo}} + \frac{32}{\text{Re}_G^2}(1+8s)^2} \quad (21)$$

(ii) $s=0$ and $\rho_s \neq 0$ for which Eq. (19) becomes

$$\text{Fr} = -\frac{8}{3} \frac{1}{\text{Re}_G} + \frac{\sqrt{2}}{3} \sqrt{\frac{\rho_p - \rho_s}{\rho_p} + \frac{32}{\text{Re}_G^2}} \quad (22)$$

and (iii) $s=0$ and $\rho_s=0$ which modifies Eq. (19) as

TABLE II. Liquid pairs and their physical properties.

Fluid	Density kg/m ³	Viscosity mPa s	Interfacial tension with water (N/m)
Water	1000	1	...
Kerosene	787	1.2	0.0385
Benzene	879	0.73	0.0356
Cyclohexane	775	0.96	0.0585
2,Heptanone	810	0.71	0.0208
Brine solution	1200	1.75	0.0378 (with kerosene)

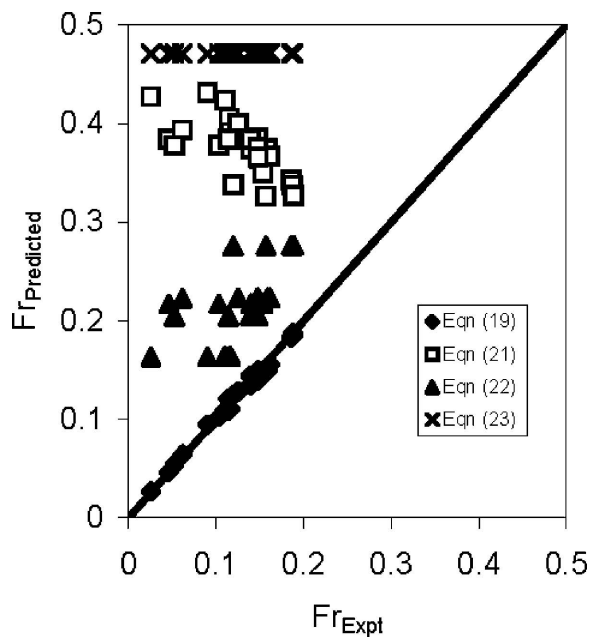


FIG. 2. Comparison of the predicted results.

$$Fr = -\frac{8}{3} \frac{1}{Re_G} + \frac{\sqrt{2}}{3} \sqrt{\frac{32}{Re_G^2}}. \quad (23)$$

A comparison between the results obtained from Eqs. (19) and (21)–(23) with experimental data is presented graphically in Fig. 2. The figure shows the remarkable improvement of the present analysis over that of Joseph¹⁸ and clearly brings out the influence of density difference and shape factor on rise velocity.

A theoretical analysis of the rise velocity of a LTB has been performed based on the assumption of viscous potential flow. The analysis accounts for the effect of density of both the liquids, viscosity of the primary liquid, and interfacial tension. The effects of viscosity and interfacial tension are incorporated in gravity Reynolds number (Re_G) and Eotvos number (Eo), respectively, while an additional term has been included to account for the density difference between the two liquids. The influence of interfacial tension totally de-

pends on the shape factor s . An accurate estimation of this factor has been obtained from image analysis.

- ¹E. E. Zukoski, "Influence of viscosity, surface tension, and inclination angle on motion of long bubbles in closed tubes," *J. Fluid Mech.* **25**, 821 (1966).
- ²A. Tomiyama, Y. Nakahara, Y. Adachi, and S. Hosokawa, "Shapes and rising velocities of single bubbles rising through an inner subchannel," *J. Nucl. Sci. Technol.* **40**, 136 (2003).
- ³D. T. Dumitrescu, "Stromung und Einer Luftblase in Senkrechten rohr," *Z. Angew. Math. Mech.* **23**, 139 (1943).
- ⁴R. M. Davies and Sir G. Taylor, "The mechanics of large bubbles rising through extended liquids and through liquids and through liquids in tube," *Proc. R. Soc. London, Ser. A* **200**, 375 (1950).
- ⁵P. R. Garabedian, "On steady-state bubbles generated by Taylor instability," *Proc. R. Soc. London, Ser. A* **241**, 423 (1957).
- ⁶H. L. Goldsmith and S. G. Mason, "The motion of single large bubbles in closed vertical tubes," *J. Fluid Mech.* **14**, 42 (1962).
- ⁷R. A. S. Brown, "The mechanics of large gas bubbles in tubes. I. Bubble velocities in stagnant liquids," *Can. J. Chem.* **2**, 217 (1965).
- ⁸D. A. Reinelt, "The rate at which a long bubble rises in vertical tube," *J. Fluid Mech.* **175**, 557 (1987).
- ⁹R. Clift, J. R. Grace, and M. E. Weber, *Bubbles, Drops, and Particles* (Academic, New York, 1978).
- ¹⁰G. B. Wallis, "General correlations for the rise velocity of cylindrical bubbles in vertical tubes," Report No. 62GL130, General Engineering Laboratory, General Electric Co., Schenectady, New York (1962).
- ¹¹G. B. Wallis, *One-Dimensional Two-Phase Flow* (McGraw-Hill, New York, 1969).
- ¹²F. Viana, R. Pardo, R. Yanez, J. L. Trallero, and D. D. Joseph, "Universal correlation for the rise velocity of long bubbles in round pipes," *J. Fluid Mech.* **494**, 379 (2003).
- ¹³F. P. Bretherton, "The motion of long bubbles in tubes," *J. Fluid Mech.* **10**, 166 (1961).
- ¹⁴K. W. Tung and J. Y. Parlange, "Note on the motion of long bubbles in closed tubes-influence of surface tension," *Acta Mech.* **24**, 313 (1976).
- ¹⁵J.-M. Vanden-Broeck, "Rising bubbles in a two-dimensional tube with surface tension," *Phys. Fluids* **27**, 2604 (1984).
- ¹⁶H. V. Nickens and D. W. Yannitell, "The effects of surface tension and viscosity on the rise velocity of a large gas bubble in a closed, vertical liquid-liquid tube," *Int. J. Multiphase Flow* **13**, 57 (1987).
- ¹⁷B. Couet and G. S. Strumolo, "The effects of surface tension and tube inclination on a two-dimensional rising bubble," *J. Fluid Mech.* **184**, 1 (1987).
- ¹⁸D. D. Joseph, "Rise velocity of a spherical cap bubble," *J. Fluid Mech.* **488**, 213 (2003).
- ¹⁹T. Funada, D. D. Joseph, T. Maehara, and S. Yamashita, "Ellipsoidal model of the rise of a Taylor bubble in a round tube," *Int. J. Multiphase Flow* **31**, 473 (2005).